

Determination of Critical Points for Reactive Mixtures: Hydrodesulfurization of 4, 6-Dimethyldibenzothiophene

M. Alvarado-Morales, E.S. Pérez-Cisneros, T. Viveros- García

^aDepartamento de Ingeniería de Procesos e Hidráulica, Universidad Autónoma Metropolitana Unidad Iztapalapa , 09430 D.F., México

A computational procedure to determine the critical points of a reactive mixture in the hydrodesulfurization of 4, 6-dimethyldibenzothiophene (4, 6-*DiMeDBT*) with tetralin as a solvent, has been developed. The critical point for a mixture of specified composition is the set of conditions (e.g. T and P) at which the mixture and the equilibrium phase have identical composition and density. Therefore, for reacting mixtures undergoing a kinetically controlled reaction process, points on the phase boundary at “close to critical” conditions are characterized by nearly identical phase compositions and phase densities. The hydrodesulfurization of 4, 6-dimethyldibenzothiophene reaction is carried out in a reactive batch distillation process. The thermodynamic analysis considers the simultaneous calculation of the reactive and non-reactive residue curve maps (Viveros-García et al., 2006) and the critical points are obtained using the Heidemann and Khalil method (Heidemann and Khalil, 1981).

Keywords: critical point, HDS, reactive distillation

Introduction

In general, there are two possible reaction paths for sulfur removal from the organo-sulfur compounds, as illustrated for 4, 6-dimethyldibenzothiophene (4, 6-*DiMeDBT*) in Figures 1. The first route is the sulfur atom direct extraction (hydrogenolysis) from the sulfured molecule. The second path is the hydrogenation of one aromatic ring followed by the sulfur atom extraction. From experimental results (Vanrysselberghe et al., 1998), it has been shown that 4, 6-*DiMeDBT* is less converted and more hydrogenated prior to sulfur removal and dibenzothiophene (*DBT*) is the most reactive in the hydrodesulfurization (HDS) reactions. Commonly, when alkyl substituents are attached to the carbon atoms adjacent to the sulfur atom, the rate for direct sulfur extraction is diminished whereas the sulfur removal rate via the hydrogenation route is relatively unaffected. Co-Mo catalysts desulfurizes primarily via the direct route, while the Ni-Mo catalyst does it via the hydrogenation route. The extent to which a given catalyst acts via one route or the other is determined by the H_2 and H_2S partial pressures and the hydrocarbon feed properties.

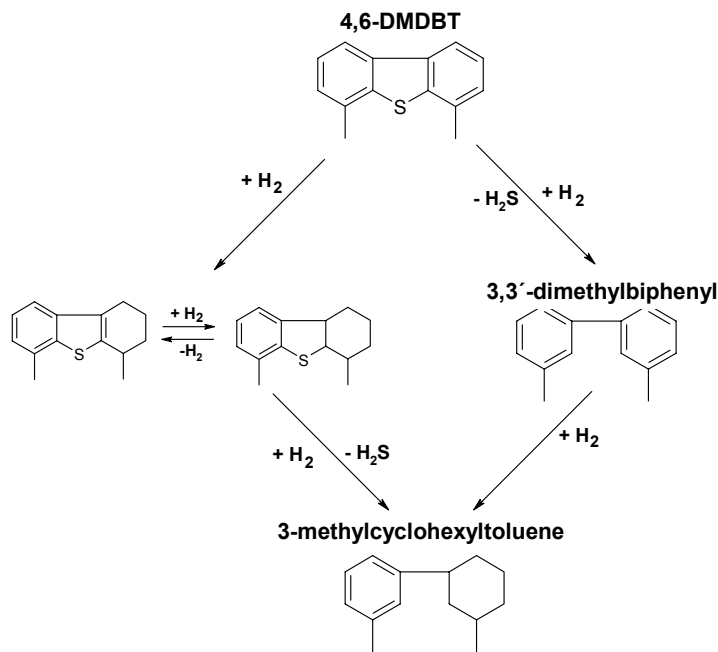
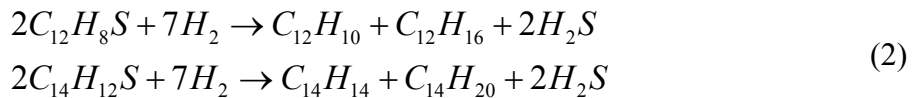


Figure 1: Reaction pathways for 4, 6-dimethylbenzothiophene hydrodesulfurization

According with the reaction networks described above, at following unbalanced hydrogenolysis-hydrogenation reactions should be carried out:



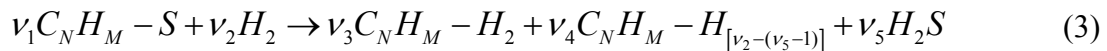
where *BPH*, and *3, 3'-DiMeBPH* are the hydrogenolysis reaction products and *CHB*, *3-MeCHT* are the hydrogenation reaction products, respectively. The above unbalanced reactions can be written in a balanced form as:



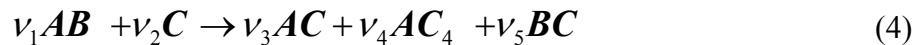
In the above reaction schemes, potential side reactions, as hydrogenation of byphenils, cyclohexylbenzenes and cyclohexyltoluenes are considered negligible in comparison with the hydrogenolysis and hydrogenation of dibenzothiophenes (Broderick and Gates, 1981; Vanrysselberghe et al., 1998).

Graphical Visualization of the Reactive Space

For the analysis of the reactive system, hydrodesulfurization reactions of the various species given by Eq. (2) may be lumped into the following general reaction:



where ν_i is the stoichiometric coefficient of compound i in the reactive mixture, $C_N H_M$ is the organic part of the organosulfur compound, $C_N H_M - H_2$ and $C_N H_M - H_{[\nu_2 - (\nu_5 - 1)]}$ are the hydrogenolysis and hydrogenation reaction products, respectively. It can be noted that the hydrogenolysis-hydrogenation reactions given by Eq. (3) involve nine different species including the solvent. Such reactions are carried out in a mixture of many hydrocarbons as solvent medium, for example, a paraffinic blend of C₁₀–C₁₆. The computation and visualization of the phase behavior of this multicomponent reactive mixture may be difficult. This is because of the complexity of the reactive mixture containing H_2 and H_2S , and the lack of experimental values for some thermodynamic properties of the organo-sulfur compounds. In order to simplify the visualization of the reactive phase behavior, it is possible to manage the hydrogenolysis-hydrogenation reactions for each organo-sulfur compound separately. Assuming a reactive mixture with only one organo-sulfur compound (i.e. DBT) and an inert species as solvent (i.e., terraline), and using the *element* concept proposed by Pérez-Cisneros et al., (1997), a reduction of the composition space is possible. Defining the following *element* representation: $A = C_N H_M$; $B = S$ and $C = H_2$, the generalized reaction (3) can be written as:



where AC and AC_4 represents all products obtained in the hydrogenation reactions from all the organosulfur compounds AB studied here. Furthermore, considering that these liquid phase chemical reactions are carried out in a solvent medium, such solvent is introduced as *element* D . With the above *element* fraction definition, the nine different species participating in the hydrodesulfurization reactions are located in this reactive phase diagram. Also, if the solvent concentration is kept constant ($W_D = \text{constant}$), different normalized planes for the reactive mixture could be sketched (see upper plane in Figure 2).

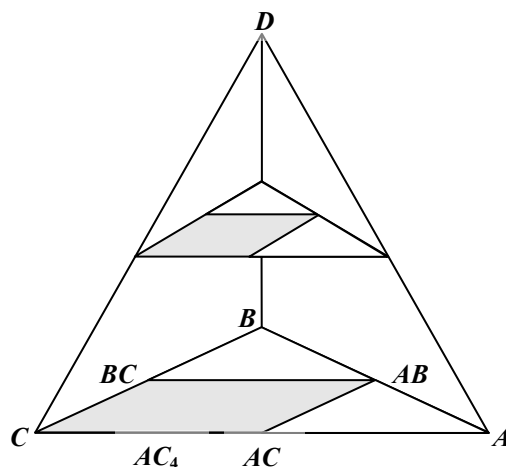


Figure 2: Three-dimensional *element* composition space for HDS of diesel

The Simple Reactive Distillation Process

Considering a simple non-reactive batch distillation process shown in Figure 3 (assuming no catalyst present), the component mass balances can be written as:

$$\frac{dx_i}{dt} = \frac{\bar{V}}{L}(x_i - y_i) \quad (5)$$

where L is the molar liquid hold-up and \bar{V} is the molar vapor flow rate. The quotient L/\bar{V} is controlled via the heating input Q , and in this case it may be assumed that the heating strategy is such that:

$$\frac{L}{\bar{V}} = \frac{L_0}{V_0} = \text{constant} \quad (6)$$

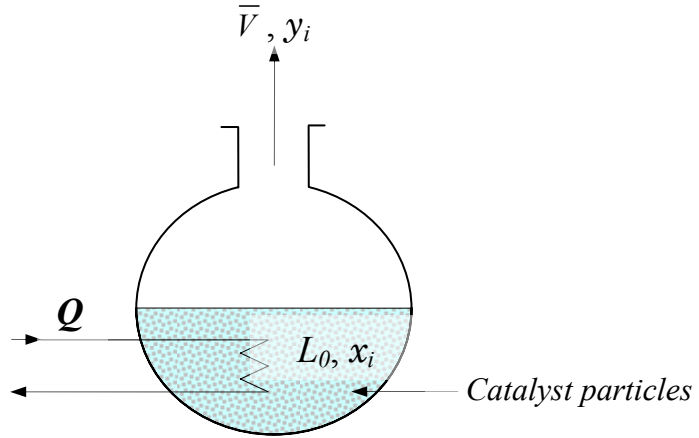


Figure 3: Simple reactive distillation process

This heating policy is physically significant and it leads to an autonomous ordinary differential equations model (Venimadhavan *et al.*, 1994). Substitution of Eq. (6) into Eq. (5) gives:

$$\frac{dx_i}{d\tau} = (x_i - y_i); \quad \text{with} \quad d\tau = \frac{L_0}{V_0} dt \quad (7)$$

The Eq. (7) represents the variation of the liquid composition in the still, when no reaction is occurring, with respect to a “warped” time. It is clear that, as the time is running, the liquid composition in the pot will be richer in the heaviest compounds since the most volatile species will leave out with the vapor flow. By the sequential integration of Eq. (7) a set of equilibrium composition points are obtained and the resulting curve that describes the liquid compositions is called a *non-reactive residue*

curve. The equations to compute the *reactive* residue curves are similar to those for the non-reactive case, but, the reaction term must be added into the mass balances and a reaction kinetic expression has to be used to compute such curves. The autonomous differential equations for computation of the reactive residue curves can be written as:

$$\frac{dx_i}{d\tau} = x_i - y_i + \alpha \sum_{j=1}^{NR} \left\{ \left[v_{ij} - \left(\sum_{k=1}^{NC} v_{kj} \right) x_i \right] \frac{r_j}{r_0} \right\} \quad (8)$$

Where α is a dimensionless reaction-separation parameter given by

$$\alpha = \frac{M_{cat} r_0}{\bar{V}_0} \quad (9)$$

In Eq. (8) NC is the number of components participating in reaction j , NR is the number of reactions, M_{cat} is the catalyst mass (kg), \bar{V}_0 is the vaporization flow (kmol/h), r_j is the intrinsic rate of reaction j (kmol/kg cat. h), r_0 is a reference rate of reaction (in this work 1×10^{-7} kmol/kg cat. h) and v_{ij} is the stoichiometric coefficient of compound i in reaction j . The reaction-separation parameter α indicates the ratio between the catalyst loaded in the distillation vessel (i.e., total wetted reacting area) multiplied by the reference rate of reaction to the vaporization flow. To carry out the integration of Eq. (8) it is necessary to calculate: *i*) the phase equilibrium and *ii*) the reaction terms. One of the problems in the phase equilibrium calculations for the hydrodesulfurization reactive system is the lack of experimental information of the critical properties and acentric factor for 4, 6-*DiMeDBT* compound and its respective hydrogenolysis and hydrogenation reaction products. Nevertheless, estimated values for these properties by using any of the group contribution methods can be obtained (Viveros-García et al., 2005). In the present work, the critical properties and acentric factors were estimated using the Joback and Reid (1987) method for *DBT* and 4, 6-*DiMeDBT*, and their respective hydrogenolysis and hydrogenation reaction products. With these estimated properties it is possible to compute the required fugacity coefficients and, to determine the phase equilibrium behavior of the reactive mixture; the original Peng-Robinson (1976) equation of state with the appropriate binary interaction coefficients was used. For the computation of the reaction terms in Eq. (8), the kinetic models for hydrogenolysis (σ catalytic sites) and hydrogenation (τ catalytic sites) reactions of dibenzothiophene, and alkyl substituted dibenzothiophenes reported by Broderick and Gates (1981) and Vanrysselberghe et al., (1998), respectively, were used. That is:

for Dibenzothiophene:

$$r_{DBT,\sigma} = \frac{k_{DBT,\sigma} K_{DBT,\sigma} K_{H_2,\sigma} C_{DBT} C_{H_2}}{\left(1 + K_{DBT,\sigma} C_{DBT} + K_{H_2S,\sigma} C_{H_2S}\right)^2 \left(1 + K_{H_2,\sigma} C_{H_2}\right)} \quad (10)$$

$$r_{DBT,\tau} = \frac{k_{DBT,\tau} K_{DBT,\tau} K_{H_2,\tau} C_{DBT} C_{H_2}}{\left(1 + K_{DBT,\tau} C_{DBT}\right)} \quad (11)$$

and for 4, 6-Dimethyldibenzothiophene:

$$r_{4,6\text{-}DiMeDBT,\sigma} = \frac{k_{4,6\text{-}DiMeDBT,\sigma} K_{4,6\text{-}DiMeDBT,\sigma} K_{H_2,\sigma} C_{4,6\text{-}DiMeDBT,\sigma} C_{H_2}}{\left(1 + K_{4,6\text{-}DiMeDBT,\sigma} C_{4,6\text{-}DiMeDBT} + \sqrt{K_{H_2,\sigma} C_{H_2}}\right)^3} \quad (12)$$

$$r_{4,6\text{-}DiMeDBT,\tau} = \frac{k_{4,6\text{-}DiMeDBT,\tau} K_{4,6\text{-}DiMeDBT,\tau} K_{H_2,\tau} C_{4,6\text{-}DiMeDBT,\tau} C_{H_2}}{\left(1 + K_{4,6\text{-}DiMeDBT,\tau} C_{4,6\text{-}DiMeDBT} + \sqrt{K_{H_2,\tau} C_{H_2}}\right)^3} \quad (13)$$

where k_{ij} is the apparent reaction rate constant for species i in catalytic sites j , K_{ij} is the adsorption parameter for species i in catalytic sites j and C_i is the concentration of species i .

Computation of Critical Points for the Reactive Mixture

The computation of the critical points is carried out through the algorithm shown in Figure 4.

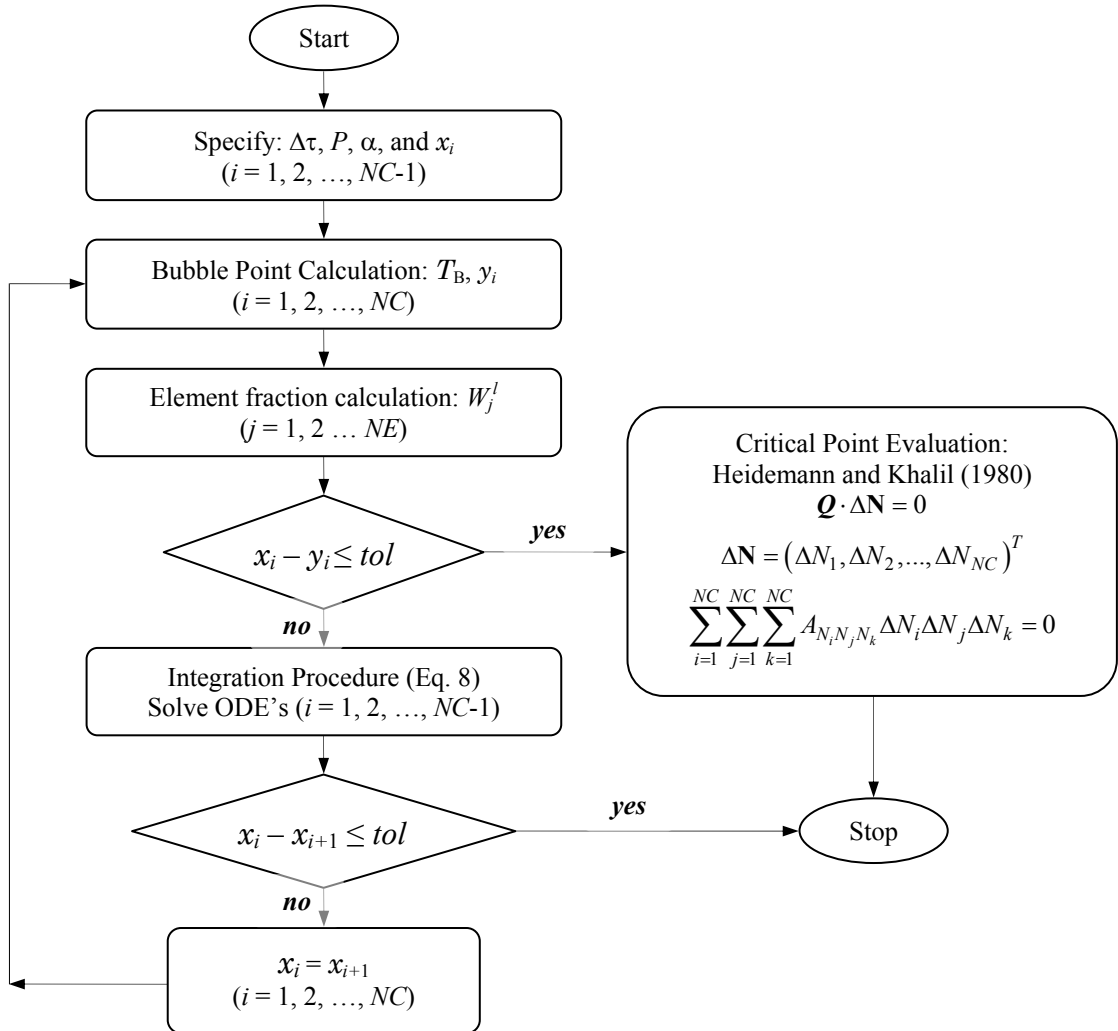


Figure 4: Algorithm for Critical Points Calculation of a Reacting Mixture

To compute the non-reactive and reactive residue curves, an initial point close to the left corner on the triangular diagram was chosen. This initial point represents the composition of a “sulfured” diesel with mole fractions: 0.0005 for *DBT* or 4, 6-*DiMeDBT* (**A**), 0.005 for H_2 (**C**) and 0.9945 for tetraline (**D**), and it is assumed that no reaction products are present. These initial mole fractions correspond to the following *element* fractions: $W_A^{0^*} = W_B^{0^*} = 9.695 \times 10^{-4}$, $W_C^{0^*} = 3.393 \times 10^{-2}$, $W_D^{0^*} = 0.96413$ and their normalization (considering constant $W_D^{0^*} = 0.96413$) gives: $W_A^0 = W_B^0 = 0.02703$, $W_C^0 = 0.94594$ (see Figure 5). These normalized *element* fractions allow to locate the initial point in the element phase diagram near to the **C** node (pure H_2). Also values for the operating pressure and the reaction-separation parameter α must be given. With the above specifications a bubble point (*T*) calculation is performed and the corresponding element fractions are evaluated. After that, a testing step over the liquid and vapor composition vectors is performed. If the composition differences are smaller than a tolerance (*tol* = 1E-10), then a critical point evaluation through the Heidemann and Khalil method is verified.

According to the methodology proposed, several simulations at different operating pressures (10, 15, 20, 25 and 30 atm) were done. At $P = 30$ atm several critical points for the reactive mixtures were identified, as can be observed in Figure 5. On the other hand, it can be observed in Figure 5 that, for values of $\alpha \leq 10$, all curves point to a binary critical point in terms of *elements*.

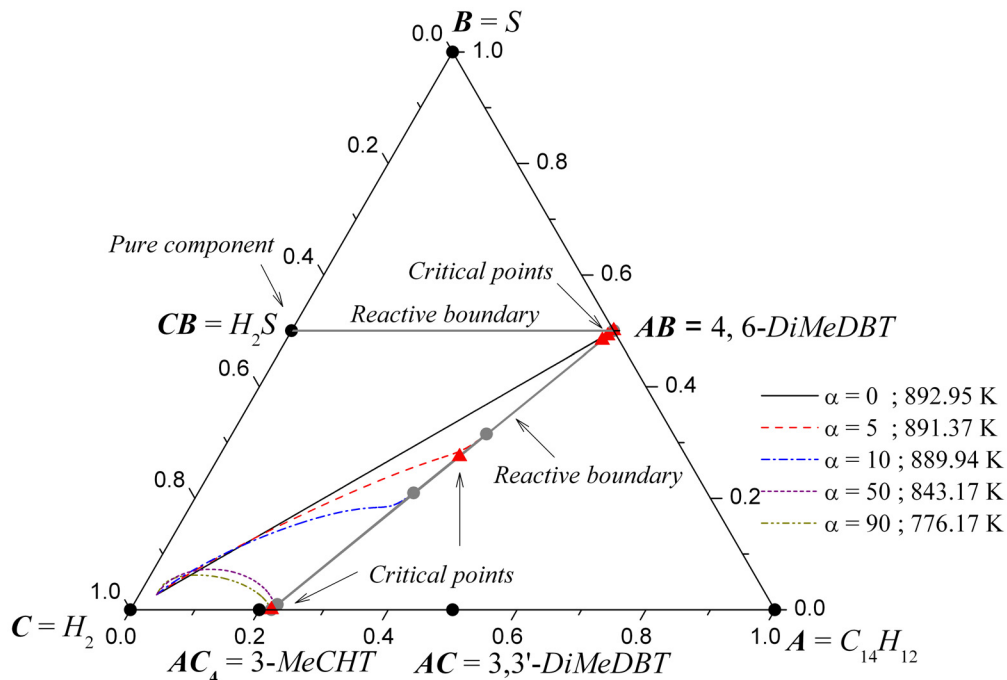


Figure 5: Location of critical points for the HDS of for 4, 6-*DiMeDBT* reactive system at $P = 30$ atm.

If the α value is augmented ($\alpha = 90$) the reactive residue curve moves close to the 3-MeCHT reaction product, and it ends at another critical point. Therefore, in absence of hydrogen in the liquid phase (AC_4 node, in Figure 5), the increment of catalyst loading, leads the reactive system to critical conditions, where the distinction between the phases is not possible. In this way, at $P = 30$ atm, the temperature region as well as the catalyst loading should be carefully considered for the design of a reactive section in a reactive distillation column, due to the critical points presence.

Conclusions

A computational procedure to determine the critical points of a reactive mixture in the hydrodesulfurization of 4, 6-dimethyldibenzothiophene (4, 6-DiMeDBT) with tetralin as a solvent, has been developed. At $P = 30$ atm several critical points for the reactive mixtures were identified. It was found that the key parameters that influence the existence of critical points are the catalyst loading and the solvent. It should be clear that the critical points are evaluated considering only phase equilibrium, that is, the reactive system is kinetically controlled.

References

- Peng, D. Y. and Robinson, D. B., (1976) *Industrial & Engineering Chemistry Fundamentals*, 15, 59-64.
- Heidemann, R.A., and Khalil, A.M., (1980) *American Institute of Chemical Engineers Journal*, 5, 769-779.
- Broderick, D. H., and Gates B. C., (1981) *American Institute of Chemical Engineers Journal*, 27, 663-673.
- Jobak, K. G., M. Thesis, Massachussets Institute of Technology, Cambridge, Mass., U. S. A. (1984).
- Pérez-Cisneros, E.S., Gani, R., and Michelsen, M.L., (1997) *Chemical Engineering Science*, 52, 527-543.
- Viveros-García, T., Ochoa-Tapia, J.A., Lobo-Oehmichen, R., de los Reyes-Heredia, J.A., and Pérez-Cisneros, E.S., (2005) *Chemical Engineering Journal*, 106, 119-131.
- Vanrysselberghe, V., Le Gall, R., and Froment, G.F., (1998) *Industrial & Engineering Chemistry Research*, 37, 1235-1242.